SINGLE STRANDED DNA:
A NEW MODEL SYSTEM FOR SINGLE MOLECULE POLYMER DYNAMICS

BY

CHRISTOPHER A. BROCKMAN

THESIS

Submitted in partial fulfillment of the requirements
for the degree of Master of Science in Chemical Engineering
in the Graduate College of the
University of Illinois at Urbana-Champaign, 2011

Urbana, Illinois

Adviser:

Professor Charles M. Schroeder

Abstract

The study of polymer dynamics has been an active area of research for many years. For nearly two decades, fluorescently-labeled double stranded DNA (dsDNA) has been the model system for studying single molecule polymer dynamics in non-equilibrium conditions. However, dsDNA is a semiflexible polymer with markedly different local molecular properties compared to flexible polymer chains, such as synthetic organic polymers. In this work, we developed a new model system for single molecule studies of flexible polymers based on single stranded DNA (ssDNA). Using a biochemical synthesis scheme called rolling circle replication, long strands (>25 μm) of ssDNA containing "designer sequences" have been generated to prevent intramolecular base pairing. Polymer chains are synthesized with amine modified bases incorporated along the backbone to facilitate labeling with fluorescent dyes. As proof-of-principle demonstration of this new chemical platform, we use epifluorescence microscopy to image individual ssDNA molecules stretching in an extensional flow generated inside a microfluidic device. It is anticipated that the model polymer system presented here will serve to promote further investigations of flexible polymer dynamics at the molecular level.

Acknowledgements

I would like to thank Dr. Charles Schroeder for giving me the opportunity to work on such an interesting project and for assisting me through any hard times. I'd also like to thank Sun Ju Kim for her work in the earlier stages of the project, and Dr. Paul Kenis for access to his clean room. Dr. Melikhan Tanyeri provided me with a great deal of information and assistance regarding the microscopy setup. Finally, I'd like to thank Amanda Marciel and Parul Koul for their help in troubleshooting certain aspects of the synthesis scheme.

This work was funded by an NIH Pathway to Independence (PI) Award, under Grant No. 4R00HG004183-04.

Table of Contents

Chapter 1
Introduction

1.1 Overview

Polymer molecules exhibit complex behavior upon deformation and exposure to non-equilibrium conditions. Polymer chains stretch and orient in solution-based fluid flows, which gives rise to flow-dependent material properties such as bulk stress and viscosity. Ultimately, the macroscopic response of a polymeric material is determined by the underlying microstructure and molecular properties of deformed polymer chains. Polymer dynamics has been studied using a wide array of experimental and theoretical tools[1, 2]. Single molecule techniques allow for the direct observation of chain dynamics at the molecular level, thereby enabling characterization of polymer backbone motion and chain stretching dynamics. Increased understanding of these phenomena can lead to improvements in polymer processing and aid in applications such as polymer solution based turbulent drag reduction.

1.2 Single Molecule Studies of λ-DNA

Over the last 15 years, double stranded DNA (dsDNA) has served as the model system to study single molecule polymer dynamics using fluorescence microscopy[3]. In particular, single molecule experiments have almost exclusively relied on lambda (λ-) DNA as a model system. Lambda DNA exhibits several advantages as "model" polymer, including facile sample preparation and fluorescent labeling. Additionally, monodisperse samples of λ-DNA are readily available from commercial vendors. A myriad of single molecule experiments have been performed using λ-DNA including chain relaxation[4], coil

diffusion[5], stretching in uniform flow[6], dynamics in extensional[7-9], shear[10] and mixed flow[11], and polymer conformation hysteresis[12]. Recently, dsDNA has been used to directly observe polymer dynamics in confined geometries[13-16].

1.3 Need for a New Polymer System for Single Molecule Studies

1.3.1 Local Flexibility

Although λ-DNA has provided useful information in single molecule studies, it is a semiflexible polymer with markedly different molecular properties compared to flexible polymer chains. In traditional hydrocarbon polymer chains, chain flexibility is determined by bond rotations about torsion angles, while the bond angle between carbon atoms remains relatively constant. The chain conformation energy depends on the torsion angle with three energy minima corresponding to the trans (0°) and gauche (±120°) states. A polymer chain is considered statically flexible if the energy difference between the trans and gauche states, $\Delta\varepsilon$, is small, i.e. $\Delta\varepsilon \approx kT$. Under these conditions, the trans and gauche states would be equally preferred at thermal equilibrium. A chain is considered dynamically flexible if the energy barrier between trans and gauche states, ΔE, is small, i.e. $\Delta E \approx kT$. When a chain is dynamically flexible, it can rapidly explore many conformations without being trapped in a narrow subset of conformation space.

The flexibility mechanisms are fundamentally different for a semiflexible polymer such as dsDNA due to the double helix structure. Double stranded DNA exhibits uniform flexibility along the entire length of the polymer backbone. The flexibility arises due to contour fluctuations[17] as opposed to torsion bond angles in flexible chains.

Semiflexible polymers are described by the worm-like chain model, and chain stiffness is determined by a parameter termed the persistence length. The persistence length is a measure of local flexibility and represents the length at which orientation persists along the chain. Double stranded DNA is relatively stiff with a persistence length of ~53 nm[18, 19], whereas polyethylene would be considered flexible with persistence length 0.57 nm[20]. This difference is further enhanced when taking into consideration labeled dsDNA, which has a persistence length of ~66 nm when stained with YOYO-1[5, 6, 21]. The chemical differences between dsDNA and a flexible polymer are illustrated in Figure 1 and demonstrate how local flexibility can alter global conformation.

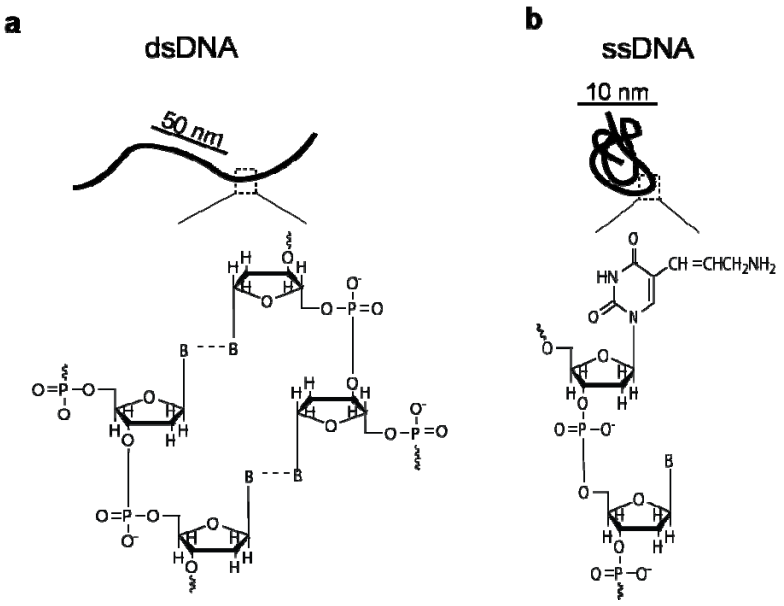

Figure 1 Polymer chain structures are shown for (a) double stranded DNA, a semiflexible polymer with a double helix backbone and (b) single stranded DNA, a flexible chain consisting of 5-carbon sugars linked by phosphodiester bonds. For ssDNA, a modified base with primary amine (aminoallyl-uracil) is shown, and 'B' represents a natural nucleobase.

1.3.2 Global Flexibility

In the past, λ-DNA has been shown to obey dynamical scaling laws for flexible polymers. This is due to the relative length scales associated with the polymer chain. In the limit of

a small persistence length relative to contour length, the chain will appear flexible at intermediate length scales longer than the persistence length. Global flexibility can be defined as the number of persistence lengths in a polymer chain:

$$\frac{L}{l_p} \sim N$$

where L is the contour length, l_p is the persistence length, and N is the number of statistical steps. Generally speaking, polymer chains with N>100 are considered globally flexible; therefore, λ-DNA is globally flexible because it contains N≈310 persistence lengths (L≈16.3μm). Although λ-DNA is considered flexible under these circumstances, the possibility arises for different dynamics for flexible polymers due to excluded volume effects or intrachain hydrodynamic effects, which arise due to local chemistry.

1.3.3 Aspect Ratio

The monomer aspect ratio describes the local asymmetry of the polymer chain and plays a role in equilibrium and dynamic chain properties. The aspect ratio, a, is defined as the ratio of the Kuhn step size, b=2l_p, to the chain diameter, d:

$$a = \frac{b}{d}$$

The aspect ratios for labeled double stranded DNA, polystyrene, and single stranded DNA are all listed in Table 1.

Table 1 Molecular properties for common model polymer chains

Parameter	dsDNA	Polystyrene	ssDNA
Aspect ratio, a	66	2	1.2
Kuhn step size, b (nm)	132	1.5	1.2
Molecular Diameter, d (nm)	2	.08	1

The monomer aspect ratio plays an important role in both excluded volume and intrachain hydrodynamic interactions. For asymmetric monomers, the ratio of the excluded volume to the occupied volume is equal to the aspect ratio[17]. If a chain has a large monomer aspect ratio, monomer-monomer interactions along the backbone are suppressed, whereas for chains with low aspect ratios monomer-monomer interactions are dominant, leading to the possibility for non-linearities in polymer chain behavior. Additionally, as the aspect ratio increases, the number of chain contacts decreases causing increasingly free- draining coil behavior when compared to nearly symmetric monomers. Free-draining coils suppress intrachain hydrodynamic interactions (HI) in the coiled state suggesting reduced importance of HI in λ-DNA. This was seen in both Brownian dynamics simulations[7, 22] and in experimental measurements of conformation hysteresis in extensional flow[12], where a 1.3 mm piece of λ-DNA was required before hysteresis in chain conformation in extensional flow was observed. Conformation hysteresis is a display of non-linear behavior that is generally suppressed in polymer chains with high aspect ratios.

1.3.4 Force Extension Measurements

In the past, the chain elasticity of synthetic polymers has generally been modeled using either the inverse Langevin (ILC) or the Warner force-extension relation[2]. The elasticity of λ-DNA and other semiflexible biopolymers has been well-described by the Marko-Siggia force-extension relation[19]. An underlying assumption for all three of these models is the absence of monomer-monomer interactions. For a force-extension relation with no monomer interactions, there is typically a linear Hookean response at low extensions:

$$x \sim f$$

where x is dimensionless extension. For polymer chains in which monomer-monomer interactions are relevant, i.e. chains with low aspect ratio, chain elasticity is non-linear at low extensions with:

$$x \sim f^{2/3}$$

This low force non-linear response was originally predicted by Pincus in 1976[23], but was only recently seen experimentally using ssDNA in a magnetic tweezer assay[24, 25]. These results further suggest that λ-DNA may not serve as a suitable "model" polymer chain for flexible polymers.

1.4 Proposed Research

The goal of the work presented in this thesis is to develop a new model system for single polymer studies of flexible chains based on single stranded DNA. In Chapter 2, rolling circle replication, a biochemical synthesis method capable of producing long strands of ssDNA, is described. Rolling circle replication (RCR) has the advantage of using template based synthesis, thereby enabling "designer sequences" of ssDNA to be generated which prevents intramolecular base pair formation. Additionally, amine-modified bases can be substituted into the reaction to serve as reactive chemical moieties for labeling along the backbone with fluorescent dyes.

Chapter 3 describes the fluorescent labeling and visualization of RCR synthesized ssDNA products. Labeled products were quantified using both traditional absorbance measurements and a nuclease assay to determine both the dye labeling ratio and to characterize the extent of dye-dye interactions. A microfluidic device was used in

combination with epifluorescence microscopy to image individual polymer chains stretching in extensional flow. Images of the stretched chains displayed clear backbones, thereby confirming the success of the biochemical labeling strategy. Chapter 4 summarizes the work and describes the challenges ahead for the application of the model system in single molecule measurements of dynamic properties such as relaxation time and stretching in extensional flow.

CHAPTER 2
Biochemical Synthesis of ssDNA: Rolling Circle Replication

2.1 Introduction

Rolling circle replication (RCR) is a method to rapidly synthesize long single stranded DNA containing many copies of tandem repeated sequences of DNA or RNA. RCR is an ideal technique for creating periodic nanoassemblies, biosensors, and repeated DNA aptamers[26]. Rolling circle replication has also been performed in a microfluidic flow system to synthesize surface-tethered DNA molecules[27]. RCR typically begins with a linear single stranded template that is hybridized to a complementary primer strand, thereby creating a circular template structure. Next, the template is ligated to form covalently closed circular ssDNA[28-30]. DNA polymerase is added and bonds to the free 3' hydroxyl group and initiates replication of the circular template. In rolling circle synthesis, DNA polymerase replicates around and traverses circular templates for hundreds to thousands of cycles, thereby generating long strands of ssDNA.

In prior studies, different experimental aspects of RCR were optimized including template size and ideal DNA polymerase[30]. Templates ranging in size from 26 to 74 nucleotides in size were all efficiently replicated using a variety of DNA polymerases. In general, mesophilic DNA polymerases were all capable of synthesizing long strands of ssDNA. In this work, phi29 DNA polymerase was used for its exceptional processivity and strand displacement activity[31, 32]. We observed phi29 to yield ssDNA products in excess of 65 kilonucleotides in length. RCR reactions were supplemented with aminoallyl

dUTP (aa-dUTP), which is a modified nucleotide containing a primary amine as a reactive chemical moiety to facilitate subsequent dye-labeling with succinimidyl ester dyes. The RCR reaction scheme used here is shown in Figure 2.

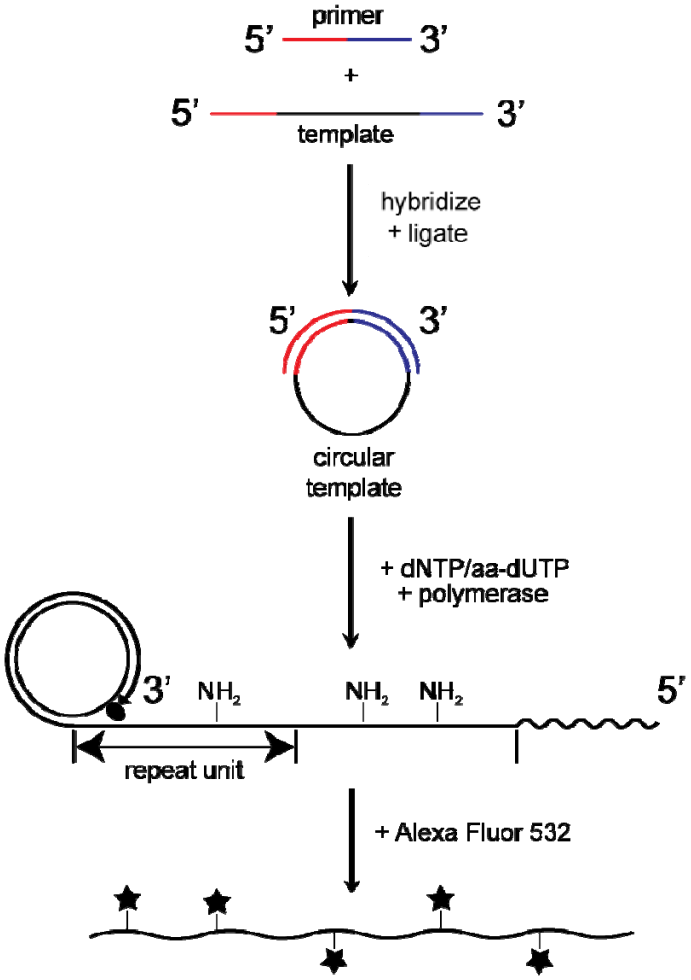

Figure 2 Schematic of rolling circle replication scheme for ssDNA synthesis. DNA polymerase is represented by an oval shape, and stars represent fluorescent dye molecules (Alexa Fluor 532).

2.2 Materials and Methods

Oligonucleotide templates and primers for rolling circle replication (RCR) were designed using VectorNTI software and synthesized by Integrated DNA Technologies (Coralville, IA). Table 2 shows the sequences of template oligonucleotides used in these experiments.

Template oligonucleotides were designed to generate ssDNA products rich in either purine or pyrimidine nucleotides. In some cases, product ssDNA was designed to be nearly homopolymeric. All template oligos contained a 5' phosphorylated terminus to enable formation of the minicircle template by ligation.

Linear templates were circularized by a ligation reaction using T4 DNA ligase (New England Biolabs). First, a reaction mixture (500 µL) consisting of 200 nM template and primer oligonucleotides in T4 DNA ligase buffer (10 mM Tris/Tris-HCl, 200 µM EDTA, 2 mM NaCl) was prepared. Template and primer oligonucleotides were hybridized by heating at 70°C for 2.5 minutes, followed by slow cooling to room temperature (20°C). Next, 600 units of T4 DNA ligase was added, and the ligation reaction proceeded for 5 hours at 16°C. In the case of Exonuclease I treatment, 20 µL (4 pmole) of the ligated/primed minicircle mixture was incubated in Exonuclease I reaction buffer (67 mM glycine-KOH, 6.7 mM $MgCl_2$, 10 mM 2-mercaptoethanol, pH 9.5) with 10 units of Exonuclease I at 37°C for 30 minutes. The Exo I enzyme was deactivated by heating to 80°C for 20 minutes. Ligated/primed minicircle templates were stored at 4°C.

RCR reactions consisted of 50 nM ligated/primed minicircle, 200 µM dTTP/aa-dUTP, 500 µM custom-mix dNTPs (containing only nucleotides in the synthesized product sequence) and 200 µg/mL BSA in phi29 DNA polymerase reaction buffer (50 mM Tris-HCl, 10 mM $(NH_4)_2SO_4$, 10 mM $MgCl_2$, 4 mM dithioethreitol, pH 7.5) in a total reaction volume of 50 µL. The polymerization reaction was initiated by addition of 5 units of phi29 polymerase, and the reaction proceeded for 30 minutes at room temperature, unless

otherwise noted. In negative control (NC) reactions, no phi29 polymerase was added. Reactions were terminated by addition of EDTA to a final concentration of 20 mM, and the products were stored at 4°C.

Gel electrophoresis was used to characterize oligonucleotide products from ligation reactions and ssDNA generated by RCR. Polyacrylamide gels (8%) were run in 1X TAE buffer (Biorad) to assay the efficiency of ligation reactions in generating ligated/primed minicircles. Polyacrylamide gels were initially equilibrated in running buffer without DNA for 20 min at 50 V, and ligated/primed oligos were loaded and run for 45 minutes at 80 V. Low molecular weight DNA ladder (NEB) was used as a standard marker. Polyacrylamide gels were post-stained with SYBR Gold (1X in TAE buffer) for 15 minutes and imaged. To assay ssDNA products from RCR reactions, agarose gels (0.6%) were run in TAE buffer using 1 kb DNA ladder (NEB) supplemented with 50 ng of λ-DNA as a standard marker. Agarose gels were run for 30 minutes at 120 V and post-stained with SYBR Gold (1X in TAE buffer) for 30 minutes. All gels were imaged using a Gel Doc 2000 (Biorad), and fluorescent gel images are inverted for display. All enzymes, including T4 DNA ligase, phi29 DNA polymerase, Exonuclease I, and DNA markers for electrophoresis and dNTP stocks were purchased from New England Biolabs. Aminoallyl dUTP (aa-dUTP) and SYBR gold were purchased from Invitrogen. All other chemicals were obtained from Sigma-Aldrich or Fischer Scientific and were molecular biology grade purity.

2.3 Results and Discussion

2.3.1 Template Design

Table 2 contains a summary of oligonucleotide template sequences and RCR reaction results. Template ssDNA sequences were designed to allow for dye labeling and to prevent intramolecular base pairing. To facilitate labeling, adenine monomers were designed to occur in template strands at semi-random locations, thereby yielding amine-modified thymine or uracil nucleotides in ssDNA product strands at tunable intervals. In addition, we designed purine-rich or pyrimidine-rich templates consisting of only 2 nucleotides (A/G or C/T), thereby preventing intrachain base pairing. In some cases, a third nucleotide (A) was present at low ratios to facilitate dye-labeling by incorporation of amine-modified nucleotides (aa-dUTP). Using this method, a wide-range of template sequences was successfully replicated by RCR, yielding long ssDNA products (>65 kb). In some cases, we observed limitations on template sequence design, as evidenced by low reactions yields or short products. In general, RCR reactions were inhibited for templates containing consecutive stretches of a single nucleotide, particularly cytosine (C) or guanine (G). Indeed, previous research has demonstrated that some polymerases are inhibited by homopolymeric sequences due to enzymatic 'slippage', and guanine-rich sequences can form quaternary structures, which may prevent ligation[32]. For some sequences, purine-rich templates failed to replicate entirely, and many of the unsuccessful reactions contained templates with larger amounts of guanine compared to the successful reactions. Overall, RCR success or failure appeared to be independent of sequence length for circular DNA templates in the range of 28-66 bases, as observed for Sequences 1-3 and Pyr 4-5.

Table 2 RCR template sequences (bold values indicate nucleotides at the primer site)

Sequence	Template Sequence	# nt	Longest 1 nt stretch	RCR success
1	5'-**ACTCTT**C(T)$_3$A(T)$_3$C(T)$_4$ACT**TTCCAT**	28	4	Yes
2	5'-**CTTTCTTA**CACT(TC)$_4$ATTC(T)$_5$AC(T)$_4$ACTTC**TTCCTACT**	48	5	Yes
3	5'-**ACTCTTTCTT**ACTTCTCTCTACTTC(T)$_6$CACTTCTCTCTAC(T)$_4$ATTTCCTT**ACCTTCTTCT**	66	6	Yes
4	5'-**AGGTGT**(G)$_4$A(G)$_4$T(G)$_4$AT**TGGATG**	28	4	Yes
5	5'-**GGTAGGTG**GT((G)$_3$AT)$_2$(G)$_3$T((G)$_3$AT)$_2$GGATGG**TGAGTGGA**	48	3	Yes
6	5'-**AGGTGAGTGGA**(G)$_4$TA(G)$_3$TT(G)$_3$T(G)$_3$A(G)$_3$TGA(G)$_3$TGGTTGGA(G)$_4$TA(G)$_3$**ATGGTGGATG**	66	4	Yes
7	5'-**AGAGGG**(G)$_{16}$**GGAGGA**	28	21	No
8	5'-**ATATTT**(T)$_7$A(T)$_8$**TTATTA**	28	10	Yes
9	5'-**ACACCCCCCC**CCA(C)$_9$A(C)$_9$A(C)$_9$A(C)$_9$ACCC**CCCCCCACCA**	66	9	No
10	5'-**ATATTTTTTT**TTA(T)$_9$A(T)$_9$A(T)$_9$A(T)$_9$ATTT**TTTTTTATTA**	66	9	Yes
Pyr 1	5'-**GGAAGA**(G)$_5$A(G)$_4$A(G)$_4$A**GAGAAG**	28	5	No
Pyr 2	5'-**AAGAGA**(G)$_7$A(G)$_7$A**GAAGGA**	28	7	No
Pyr 3	5'-**AGA(G)$_3$**GAGAGAGAGAGAGAGA**(G)$_4$AA**	28	4	No
Pyr 4	5'-**GAGGAA**GAGAGAGAGAGAGAGA**GGAAAG**	28	3	No
Pyr 5	5'-**GAGGAAGG**GAGGAGAGAGGAGAGGAGGGAGAGAGAGA**GGAGGAAA**	46	3	No
Pyr 6	5'-**GGGAGA**(A)$_4$G(A)$_7$GAAA**GGAGAA**	28	7	Yes
Pyr 7	5'-**GAGAAT**GAGGGATGAGAGGAAG**AGGAAA**	28	3	No
Pyr 8	5'-**AGGAGA**(A)$_4$G(A)$_7$G(A)$_3$**AGAAGG**	28	7	Yes
Pyr 9	5'-**GAG(A)$_7$**AAG(A)$_9$G(A)$_9$G(A)$_9$G(A)$_9$GAAA**(A)$_6$GAAG**	66	9	Yes
Pyr 10	5'-**AGGAGT**(G)$_4$A(G)$_4$T(G)$_4$AA**AGGATG**	28	4	Yes

2.3.2 Hybridization Results

Polyacrylamide gel electrophoresis (PAGE) was used to assay ligation of circular template strands. Figure 3a shows a gel image containing linear templates and ligated/primed mincircles for Sequence 10, where linear templates migrate slower than minicircles. In Lane 2, the bright band corresponds to primed minicircle templates, and the upper and lower weaker bands correspond to unreacted linear templates and unprimed minicircles, respectively. For some ligation reactions, primed minicircle templates were treated with exonuclease (Exo I), which specifically degrades linear DNA. Samples treated with Exo I show single bands on PAGE gels corresponding to unprimed closed circular ssDNA (Lane 3). Following ligation, primed minicircle templates were carried forward to 30 minute RCR reactions. Figure 3b shows an image of ssDNA products from RCR reactions analyzed using native, non-denaturing agarose gel electrophoresis. For

minicircle templates treated with Exo I, ssDNA product bands are faint due to near complete digestion of the minicircle primer, which is required for replication.

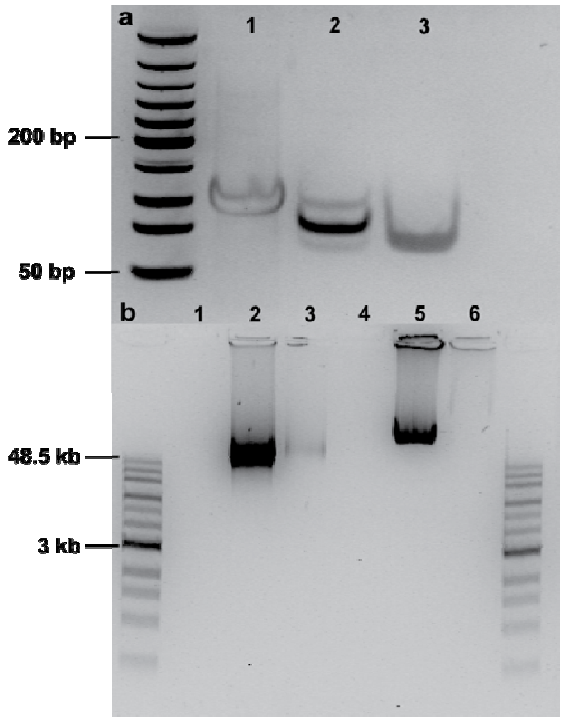

Figure 3 Rolling circle replication for ssDNA. (a) PAGE gel showing minicircle template formation (Sequence 10). Lane 1: linear template, Lane 2: ligated/primed minicircles, Lane 3: Exo I treated minicircles. (b) Agarose gel showing ssDNA products from RCR for Sequence 1 (Lanes 1-3) and Sequence 10 (Lanes 4-6). Lanes 1 and 4 are negative controls, Lanes 2 and 5 show ssDNA products generated from primed minicircle templates, and Lanes 3 and 6 show ssDNA products from Exo I treated minicircle templates.

2.3.3 Reaction Time Results

The effect of RCR reaction time on ssDNA product length distributions was characterized using Sequence 1. Figure 4 shows an image of an agarose gel containing ssDNA products from timed RCR reactions with durations ranging from 0.5 to 180 minutes. As expected, ssDNA product length increases with increasing reaction time. In addition, product bands appear to broaden and intensify for long reaction times, indicating increases in both product yield and polydispersity. Typical yields for a single

RCR reaction were on the order of 1-2 μg depending on reaction time. To increase yield for dye labeling, multiple reactions were carried out in parallel.

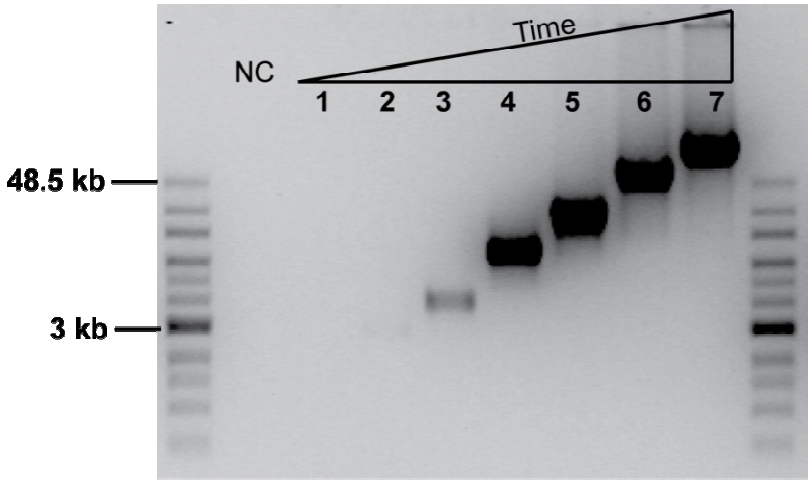

Figure 4 RCR reaction time was varied between 0.5, 2, 5, 10, 30, 60, and 180 minutes in Lanes 1-7, respectively. NC: negative control with no phi29 DNA polymerase.

2.3.4 Aminoallyl-dUTP Incorporation Results

The ratio of natural to modified nucleotide (dTTP:aa-dUTP) in the reaction mixture was varied to determine the effect of unnatural bases on product lengths (Figure 5). Upon increasing the amount of aa-dUTP, product length, yield, and polydispersity remained nearly constant, which suggests that the base modification is non-perturbative for replication by phi29 polymerase.

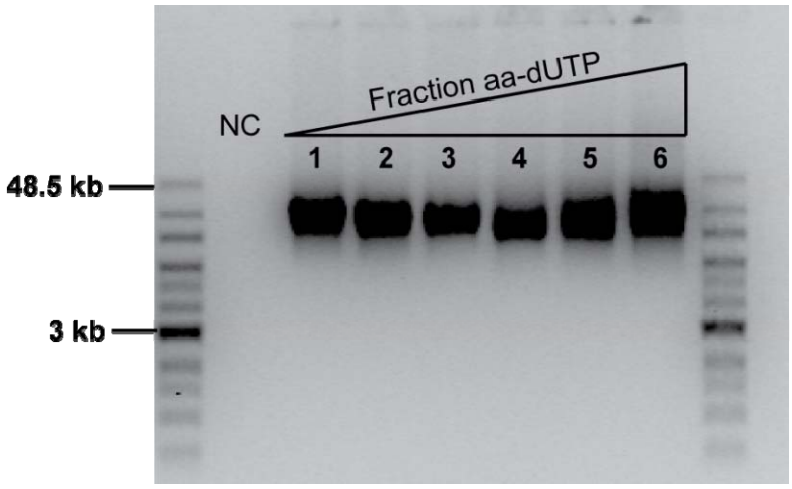

Figure 5 RCR products for varying ratios of natural to modified nucleotide, with dTTP:aa-dUTP ranging between 1:0, 4:1, 3:2, 2:3, 1:4, 0:1 in Lanes 1-6, respectively. Agarose gels (0.6%) were run for 30 min at 120V. NC: negative controls (no phi29 DNA polymerase).

Figure 6 shows alkaline agarose gel electrophoresis for ssDNA samples containing variable ratios of aa-dUTP:dTTP. Alkaline agarose gel electrophoresis was performed using standard protocols in molecular biology, and the denaturing conditions allow for accurate determination of molecular weight. The results shown in Figure 6 are consistent with those in Figure 5 in that ssDNA samples are relatively monodisperse, with the general absence of broad molecular weight distributions; however, as the fraction of aa-dUTP is increased, some amount of ssDNA product exhibits inhibited mobility in the denaturing gel, presumably due to the modified aa-dUTP nucleotide and the chemical nature of the additional primary amine. Single molecule visualization directly reveals that after dye labeling, ssDNA molecules from these samples (Sequence 1) stretch to reveal clean, linear and pristine ssDNA polymer backbones.

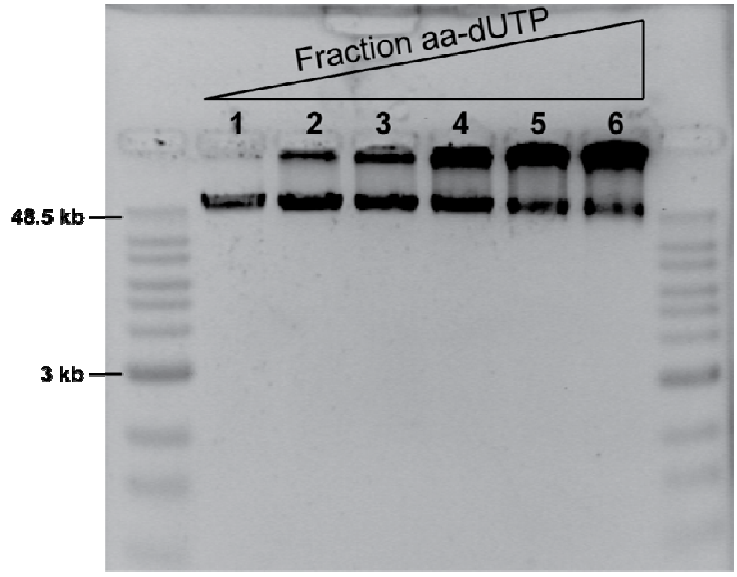

Figure 6 Denaturing alkaline gel electrophoresis for replicated ssDNA products (Sequence 1) with varying dTTP:dUTP ratios. The dTTP:dUTP ratios varied between 1:0, 4:1, 3:2, 2:3, 1:4, and 0:1 in Lanes 1-6, respectively. The lower band corresponds to ssDNA product, which shows similar molecular weight as a function of increasing dUTP. As the dUTP content was increased, some of the ssDNA product showed inhibited mobility within the gel, however, the gel conditions were denaturing, which fully prevents base pairing interactions. The gel was a 0.6% alkaline agarose gel and was run at 60V for 1 hour.

2.3.5 Pyrimidine-Rich ssDNA Product Results

As shown in Table 2, RCR reactions were performed to yield products rich in either pyrimidines or purines. In general, higher molecular weight products were obtained for ssDNA rich in purines (A/G) compared to pyrimidine rich products. For most ssDNA sequences, products migrated with similar mobility on both native and denaturing gels, suggesting the absence of base pairing in ssDNA products. Interestingly, ssDNA products rich in pyrimidine bases (generated by Sequences 4-6 and Pyr 6, 8-10) showed inhibited migration through native agarose as demonstrated in Figure 7a. For these sequences, denaturing gels were used to quantify product length distributions, in addition to single molecule visualization. Alkaline conditions (Figure 7b) enabled product migration but

demonstrated large smears over a wide range of product lengths, indicative of a large increase in polydispersity compared with purine-rich ssDNA products.

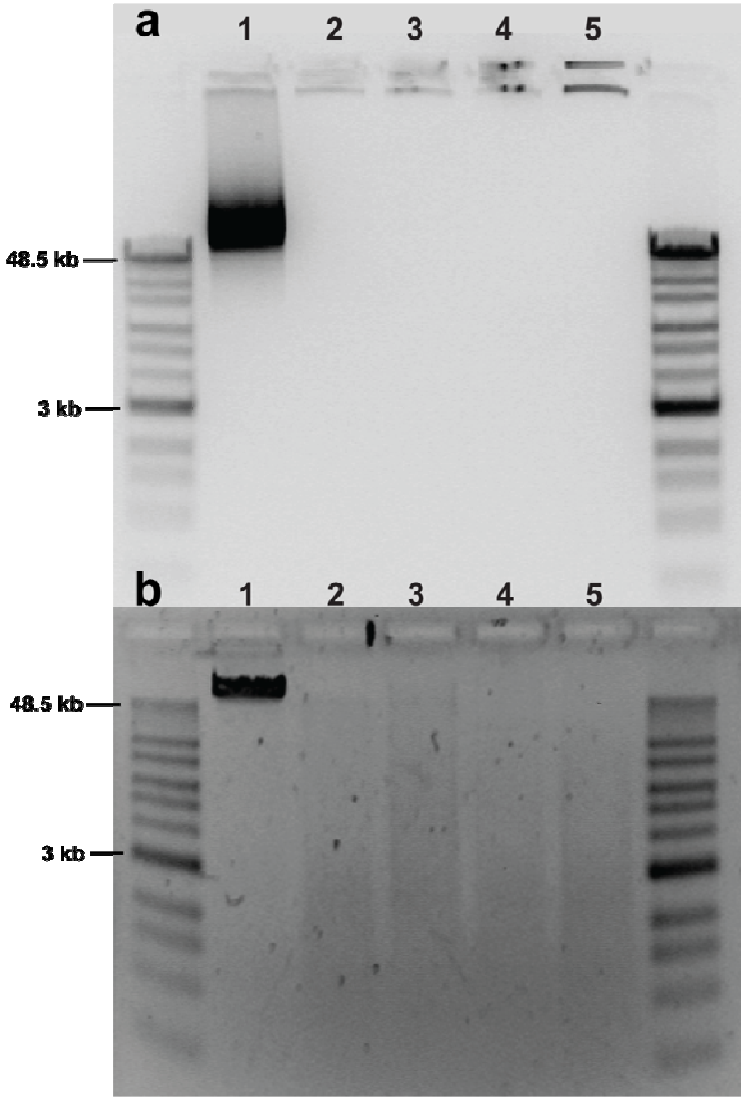

Figure 7 RCR products for Sequences 1, 4, 5, 6, and Pyr 6 in Lanes 1-5, respectively, were run in both (a) native and (b) alkaline agarose gel electrophoresis. Sequence 1 yields large ssDNA product and was used in single molecule visualization studies. Sequence 1 migrates at nearly the same mobility in native and denaturing gels, which suggests the absence of base pairing interactions. For other sequences (4, 5, 6), the gels illustrate the sequence-dependent product mobility in native agarose gel electrophoresis. In general, we observed pyrimidine-rich sequences to migrate slowly through native gels, which presumably does not arise due to base pairing, because nearly homopolymeric (dT) ssDNA also did not migrate efficiently in native gels (Lane 5, Pyr 6). Finally, these gels show the difference in product length distributions for purine-rich (Sequence 1) and pyrimidine-rich (Sequences 4, 5, 6, Pyr 6) sequences.

2.3.6 Base Pairing and Base Stacking Interactions

In this work, ssDNA sequences are designed to prevent intrachain base pairing and base stacking interactions. In nature, base stacking is an important phenomenon that aids in stabilization of the double helix in dsDNA. In ssDNA, base stacking can give rise to helical domains. Stacking interactions in ssDNA are dominant for poly(dA) and poly(dC) homopolymeric sequences, as evidenced by plateaus in AFM force-extension elasticity data for homopolymeric ssDNA molecules[33-36]. Poly(dT) shows minimal or no evidence of base stacking and exhibits force-extension curves similar to random ssDNA sequences (denatured λ-DNA)[37].

For the majority of the designer sequences (including Sequence 1), base stacking is not expected. Stacking is primarily relevant for homopolymers with long poly(dA) domains[33], which do not occur in any of the designer sequences except Sequences 8 and 10, which were not used in labeling experiments. Furthermore, base stacking interactions are weak between chemically distinct bases[33] and mainly dominate in homopolymeric sequences, which has been previously verified in molecular beacon experiments where a single base defect in a poly(dA) loop significantly impacted the enthalpic barrier to hairpin closing[38]. Base stacking involves only interactions between neighboring nucleobases and is either non-cooperative or weakly cooperative[33], which implies that short stretches of single base connected by a differing nucleotide are not impacted by base stacking.

Finally, precautions were taken to minimize or completely eliminate intramolecular base pairing in ssDNA products. By design, hairpins are avoided in all sequences used in this work. Templates for RCR were designed to be either pyrimidine-rich (C/T) or purine-rich (A/G) sequences that never contained all four nucleotides. For some pyrimidine-rich templates, a third base (A) was included in minicircles in small amounts (~1:10 bases) to facilitate labeling with aa-dUTP (e.g., Sequence 1). Base pairing energies were calculated for all sequences, and in all cases, the energy was low and on the order of thermal energy (k_bT). A single isolated dATP-dTTP base pair in a long, non-interacting chain (e.g., Sequence 1) is a relatively weak interaction with energy ~1.3 k_bT[39]. Previous work based on Monte Carlo simulations was used to model force-extension data for random and hairpin sequences (poly(dA-dT) and poly(dG-dC)) using standard base pairing rules, and random sequences did not alter the elastic chain behavior[40]. In Chapter 3, single molecule images of stretched ssDNA reveal clean and pristine linear polymer backbones, with no discernable evidence of base interactions. It is anticipated that base pairing plays no role for ssDNA molecules containing user-defined tailored sequences used in this work, in particular Sequence 1.

2.4 Concluding Remarks

This chapter presents work on rolling circle replication and demonstrates the ability of RCR to synthesize long strands of ssDNA. Rolling circle replication has advantages over other synthesis methods due to the ability to precisely control sequence composition and incorporate non-natural bases in ssDNA products. In this chapter, the effects of reaction time, non-natural base concentration, and sequence composition were all characterized. As expected, product lengths and yields both increased with increasing reaction times

(Figure 4). Additionally, the phi29 polymerase enzyme successfully incorporated modified nucleotides with no apparent decrease in product length (Figure 5). Although not all designer sequences were replicated successfully, a wide range of product compositions was obtained. These products are the starting material for fluorescently labeled flexible polymer chains. In Chapter 3, the labeling process and subsequent single molecule visualization of the RCR synthesized ssDNA is described.

CHAPTER 3
Fluorescent Labeling and Single Molecule Visualization

3.1 Introduction

In Chapter 2, the biochemical synthesis method for generating long strands of single stranded DNA was explained. This chapter discusses fluorescent labeling of ssDNA with organic dyes (Alexa Fluor 532). The labeling scheme implemented here has several advantages over base intercalation labeling methods for double stranded DNA. In the past, λ-DNA has been labeled with intercalating dyes such as YOYO-1 and the Sytox family of dyes. Although these dyes allow for single molecule imaging of dsDNA, they alter the backbone structure of the molecules and rigidify the polymer chain. In most work, the backbone is saturated with dye molecules at a rate of one dye molecule per four base pairs. Using covalent incorporation of dye molecules and via careful adjustment of the number of dye labeling sites, we believe ssDNA is labeled without alterations to backbone structure and at easily tunable dye incorporation ratios.

3.2 Materials and Methods

3.2.1 Fluorescent Dye Labeling and Quantification

Single polymer imaging experiments were performed using Sequence 1 (Table 2). RCR reaction times were increased to 90 minutes to generate long ssDNA products appropriate for single molecule fluorescence microscopy. Prior to fluorescent labeling, ssDNA from RCR reactions was mixed with guanidine hydrochloride to a final concentration of 2M to denature products and circular templates. The mixture was concentrated in a Vivacon 2 spin column and purified using a HiTrap desalting column and fast protein liquid

chromatography (AKTA FPLC, GE Biosciences), thereby removing excess oligonucleotides and dNTPs. Approximately 800 µL of the RCR reaction mixture was loaded onto the FPLC and eluted into Alexa Fluor 532 labeling buffer (100 mM sodium bicarbonate, pH 8.0)[41]. Purification and ssDNA concentration prior to labeling was performed using Vivacon2 spin columns, 100 kDa MWCO (Sartorius). Approximately 2 mL of eluted ssDNA sample was loaded onto the spin columns and centrifuged at 2,500xg for 45 minutes, which generally yielded a 25-30X increase in DNA concentration, as determined by measuring absorbance at 260 nm using a Nanodrop 1000 (Thermoscientific). Purified ssDNA (5 µg) was labeled with 2 uL of 30 µg/µL NHS-ester Alexa Fluor 532 (Invitrogen). Solutions were mixed thoroughly by pipet and the reaction proceeded for 1 hour at room temperature in the dark. In all labeling reactions, DNA and dye concentrations were maintained constant to standardize reaction conditions. Labeling reactions were quenched by addition of 1 M Tris/Tris-HCl (pH 8.0) to a final volume of 70 µL.

Following the dye labeling reaction, ssDNA products were purified from unreacted fluorescent dye to enable single molecule imaging and for quantification of dye labeling ratios. Immediately following quenching of the ssDNA labeling reactions, reaction mixtures were purified using two successive Biospin 6 columns (Biorad), which also served as a buffer exchange to elute fluorescently-labeled ssDNA products in 10 mM Tris/Tris-HCl buffer (pH 8.0). Dye labeling ratios were determined using absorbance measurements. Fluorescently-labeled ssDNA for single molecule experiments was

supplemented with EDTA (10 mM) and diluted with 50% (v/v) glycerol for storage at -20°C.

Bulk fluorescence measurements of enzymatically-digested fluorescently-labeled ssDNA were used quantify the extent of putative dye interactions (if any) along the polymer backbone. Here, 1.5 μg of labeled ssDNA sample was split into two, equal concentration reactions. One reaction treated with an excess of DNase I for 30 minutes at 37 ºC, and the second reaction was untreated. Bulk fluorescence measurements were performed by illuminating samples at excitation wavelengths between 400-540 nm, while monitoring emission at 555 nm using a Cary Eclipse Fluorescence Spectrophotometer (Varian).

3.2.2 Fluorescence Microscopy

Direct visualization of single fluorescently-labeled ssDNA molecules was performed using epifluorescence microscopy. Single stranded DNA was imaged using an Olympus IX71 inverted microscope equipped with a 100x oil immersion objective lens (Olympus UPlanSApo) and an Andor Ixon EMCCD camera. A solid-state laser (CrystaLaser) was used as an illumination source at a wavelength of 532 nm. Polymers were imaged in viewing solution containing 50 mM Tris/Tris-HCl (pH 8.0), 1 mM EDTA, 5 mg/mL glucose, 20 mM NaCl, and ~95% glycerol by weight. Prior to microscopy, solutions were purified with a 0.45 μm membrane filter, followed by addition of β-mercaptoethanol (140 mM), glucose oxidase (~65 U/mL) and catalase (1.1 kU/mL) as oxygen scavenging reagents to minimize photobleaching of the Alexa Fluor dye. For viewing, ~50 ng of fluorescently-labeled ssDNA was added to 1 mL of viewing solution (yielding ~1-10 pM ssDNA). Individual ssDNA molecules were visualized both in quiescent conditions on a

microscope slide and in planar extensional flow generated in a PDMS-based microfluidic device, which effectively stretches ssDNA molecules for backbone visualization. Images were processed using ImageJ software. All images were corrected for background, false color was applied, and in some cases, levels were adjusted to filter approximately 15-20% of the lowest intensity pixels for noise reduction.

3.2.3 PDMS Microfluidic Device Fabrication

Hybrid polydimethylsiloxane (PDMS)/glass microfluidic devices were fabricated using standard soft-lithography techniques. A schematic of the device is shown in Figure 8. Microfluidic devices were used to generate planar extensional flow. Single stranded DNA molecules are stretched and imaged in this flow field. The fluidic layer was patterned in PDMS using replica molding. The mold for the device was prepared by spin coating negative photoresist (SU-8) onto a silicon wafer (3" diameter) and patterning with UV exposure using a high-resolution transparency film as a mask. Typical photoresist layer thicknesses ranged from 10-50 μm depending on the spin conditions and photoresist used. The molds were developed using propylene glycol methyl ether acetate (PGMEA) and treated under vacuum with trichlorosilane vapor to prevent adhesion of cured PDMS. Next, PDMS with a 10:1 base:crosslinker ratio (w/w) was cast on the mold with a thickness of ~5 mm. The cast was cured for 2 hours at 70°C. After curing, the PDMS replica was peeled off the silicon mold, and inlet and outlet ports were introduced using a blunt needle. The PDMS replica with access ports was bonded to a glass coverslip via plasma oxidation to yield a functional device.

DNA molecules were imaged in the vicinity of a stagnation point in an extensional flow generated in a cross-slot device. In this way, ssDNA molecules stretched to near full extension in free solution using extensional flow, which is an effective flow field for polymer stretching and orientation. Manual trapping of single ssDNA molecules was performed using a micrometering valve connected to one of the outlet tubes. Manual adjustment of the micrometering valve allowed for real-time positioning of the stagnation point, thereby enabling trapping of single molecules. Both outlets of the device combined into a single outlet using a Y-junction and were directed into a waste tube.

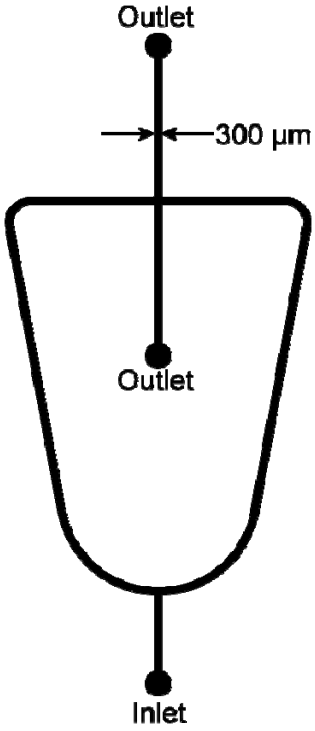

Figure 8 Schematic of the PDMS device used for stretching ssDNA. The width of the channels was 300 µm and the channel height was 50 µm.

3.3 Results and Discussion

3.3.1 Fluorescent Dye Labeling and Quantification

We desired to label ssDNA with low amounts of fluorescent dye in order to allow for efficient visualization of single polymers, while also minimizing putative modifications to the native ssDNA backbone. For determination of optimal backbone labeling, three batches of ssDNA (Sequence 1) were synthesized with varying amounts of aa-dUTP, specifically with aa-dUTP:dTTP ratios of 1:9, 3:7, and 3:2. All three samples were labeled with dye, purified and analyzed using bulk and single molecule techniques.

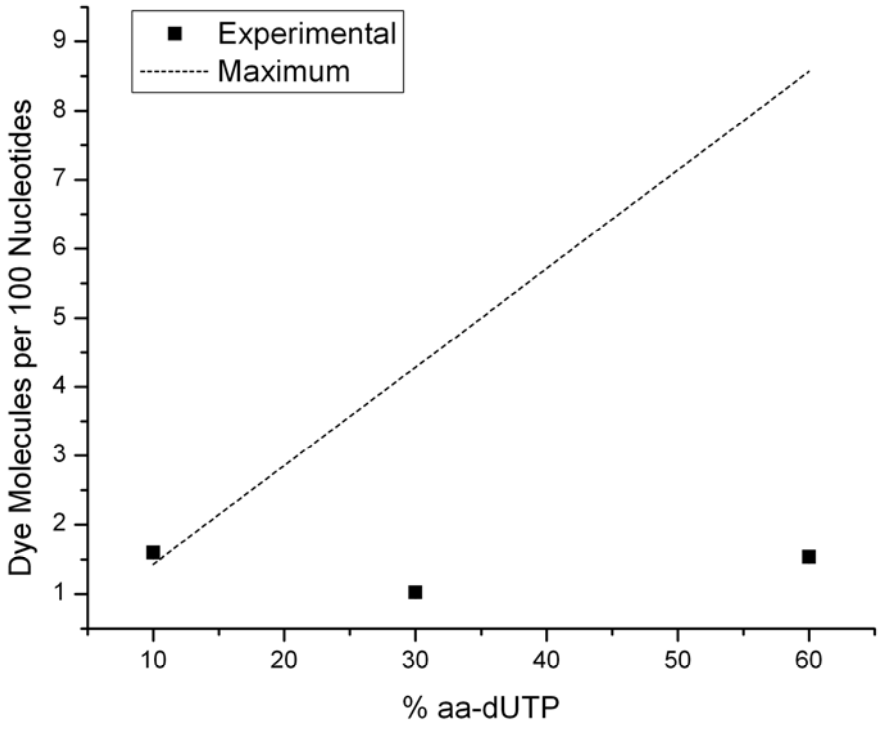

Figure 9 Summary of dye labeling ratios as a function of aminoallyl-dUTP ratio. Error bars are minimal and are contained within the size of the data labels.

Figure 9 contains the results for the dye labeling ratio measurements. The number of dye molecules per 100 bases was experimentally determined using UV and visible wavelength absorption measurements. The theoretical maximum dye labeling ratio was determined by assuming stoichiometric incorporation of aa-dUTP and quantitative completion of the labeling reaction. In general, each sample had a dye labeling ratio less than the theoretical maximum, though we determined similar labeling ratios for all samples (~1 dye:100 bases). However, bulk fluorescence data and single molecule experiments suggest that ssDNA molecules become moderately (~2x) brighter upon increasing amounts of aa-dUTP. One possible explanation is incomplete removal of unincorporated dye molecules. Experimentally measured dye-labeling ratios represent maximum labeling amounts for chain backbones and serve as an effective upper limit for dye incorporation. Overall, a labeling ratio of ~1 dye:100 bases is low and significantly less than the typical labeling ratio for dsDNA (1 dye:4 bp) using intercalating dyes such as YOYO-1.

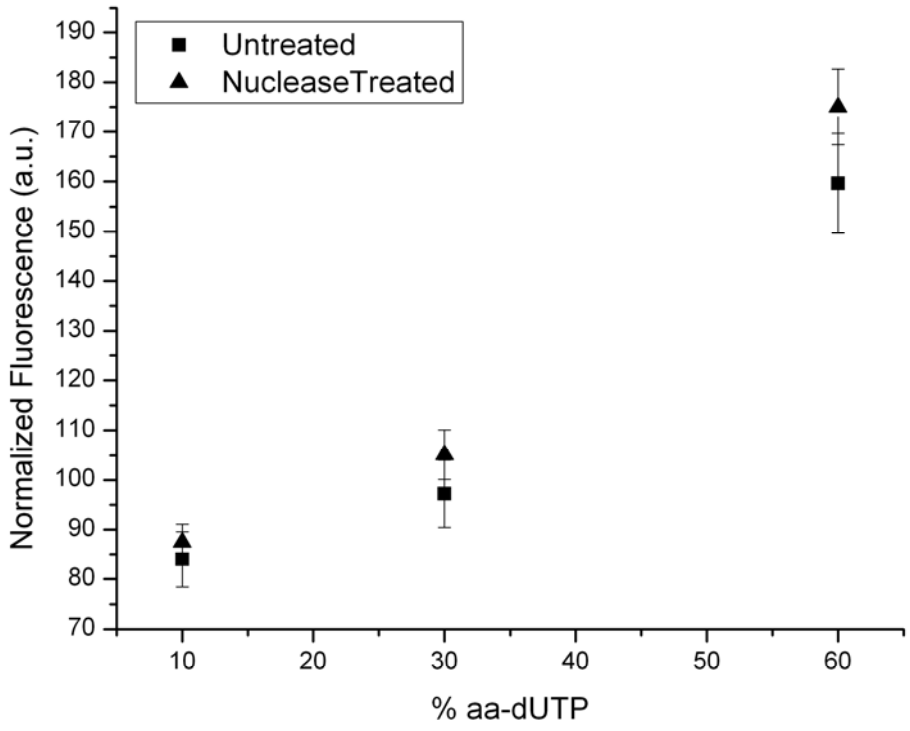

Figure 10 Fluorescent measurement results for labeled ssDNA samples with varying amounts of aminoallyl-dUTP. Three measurements of each sample were taken with a standard deviation shown by the error bars. All measurements had background subtracted as determined by monitoring the emission fluorescence at excitation ranges outside the excitation range of the dye.

Bulk level fluorescence measurements in combination with a nuclease assay were utilized to probe for putative dye-dye interactions arising from pi bond stacking for dye molecules along the polymer backbone. The results are shown in Figure 10. The nuclease assay showed no dye interactions, as measurements before and after nuclease treatment were within error measurements. This was expected because the degree of labeling for ssDNA polymers was low (~1 dye:100 bases) and far below labeling amounts for previously observed dye-dye interactions using Alexa fluorophores of ~8 dyes:100 bases[42].

3.3.2 Epifluorescence Microscopy

Fluorescence microscopy was used to directly image single fluorescently-labeled ssDNA molecules. Single ssDNA molecules generated by RCR synthesis are bright, photostable and suitable for single molecule fluorescence microscopy (Figure 11). Images of fluorescently-labeled ssDNA were directly compared to images of λ-DNA labeled with an intercalating dye. Currently, λ-DNA is the standard molecule for single molecule polymer studies, and this comparison serves as a useful benchmark for fluorescent labeling studies. Single λ-DNA molecules were labeled with YOYO-1 as described elsewhere, and dsDNA was imaged using epifluorescence microscopy using a mercury lamp as the illumination source.

Figure 11 shows images of stretched and coiled ssDNA molecules (Sequence 1) for ssDNA samples with variable dye loadings, with a side-by-side comparison to fluorescently-labeled λ-DNA. Polymer molecules are stretched using a microfluidic flow device, as described in the materials and methods section 3.2.3 of this chapter. Stretched ssDNA molecules were chosen to be of similar length to stretched λ-DNA (~20 μm contour length for stained DNA). Clearly, fluorescently-labeled ssDNA molecules appear as bright polymer chains suitable for single molecule visualization. Overall, the ssDNA sample synthesized with a 3:2 ratio of aa-dUTP:dTTP showed comparable image quality to λ-DNA. Chain backbones appeared brighter, and the signal to noise levels for labeled ssDNA molecules improved as the aa-dUTP:dTTP ratio was increased, which is generally consistent with the fluorescence data in Figure 10. Overall, these experiments serve as a useful guide to generate ssDNA for single molecule studies.

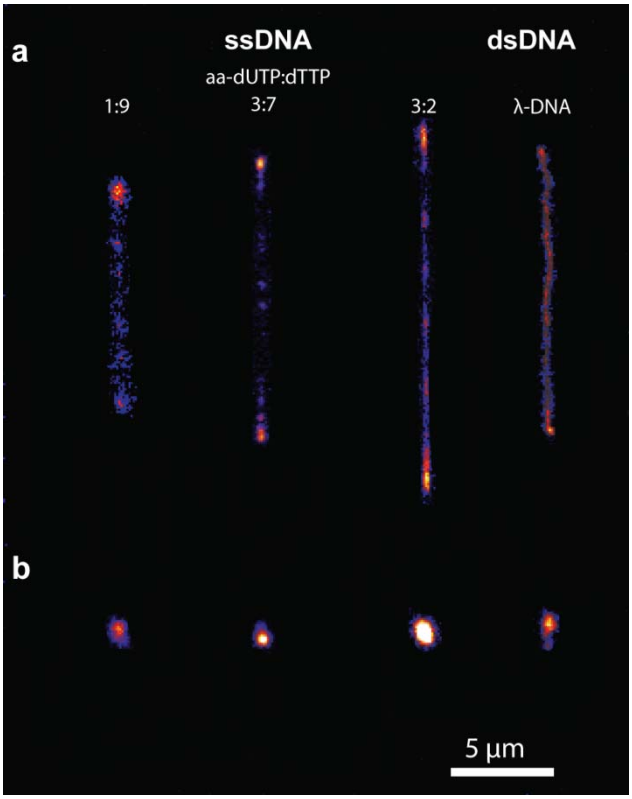

Figure 11 Direct visualization of fluorescently-labeled ssDNA molecules using fluorescence microscopy. Single molecules of ssDNA and ds-λ-DNA are shown for (a) stretched and (b) coiled configurations. ssDNA (Sequence 1) with variable dye-labeling ratios are imaged.

As discussed in Chapter 2, using rolling circle synthesis to generate long pieces of ssDNA results in polydisperse ssDNA products. To estimate chain length distributions in replicated ssDNA samples, pulsed field gel electrophoresis (PFGE) was used. Pulsed field gel electrophoresis increases the size resolution of DNA fragments as compared to native gel electrophoresis by switching the polarity of the electric field between the electrodes. In this manner, DNA moves in both forward and reverse directions in the gel, thereby resulting in enhanced separation of larger samples [43]. The results (not shown) illustrated that ssDNA (Sequence 1) synthesized by RCR using 60 minute reactions produced chains with an average size of ~50 kbases. To further quantify sample

polydispersity, single ssDNA molecules stretched to near full extension were directly visualized using fluorescence microscopy. Chain length distributions and a histogram of ssDNA molecule size was constructed (Figure 12). In particular, ssDNA polymers were stretched in a stagnation point flow generated in a PDMS-based microfluidic device, which is a useful method for stretching polymers to high degrees of extension (~90% contour length). Polymer length was determined by measuring chain end-to-end distance using image analysis.

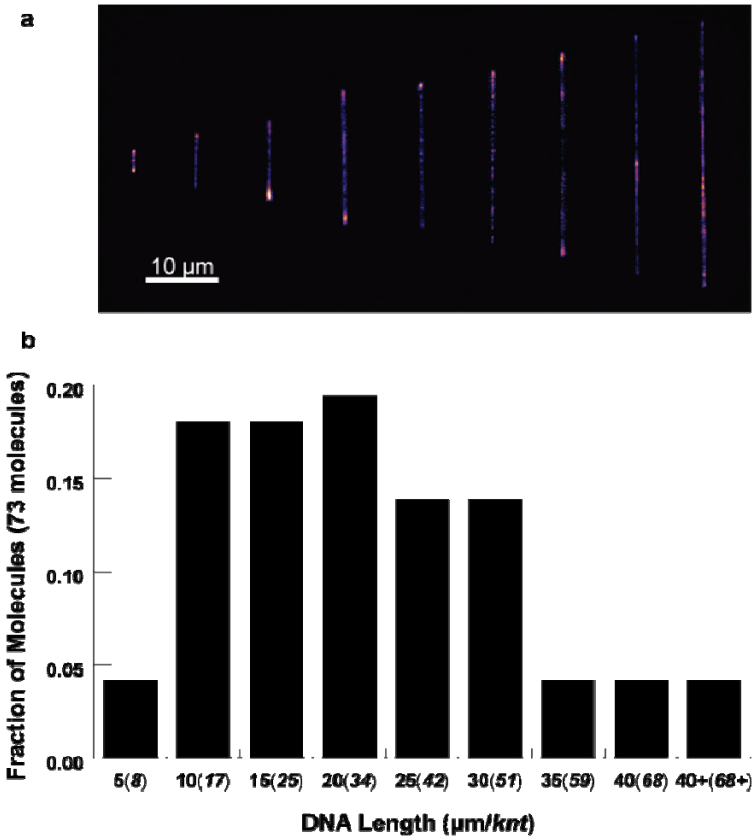

Figure 12 Histogram of ssDNA size distribution using single molecule visualization. (a) Single ssDNA molecules are classified based on size[34, 44] and binned into (b) size distributions over a 73 molecule ensemble.

As shown in Figure 12, the majority of ssDNA molecules were sized larger than ~20 µm (equivalent to the contour length of stained ds-λ-DNA), in agreement with PFGE

analysis. Additionally, ~10-15% of molecules exhibited stretched lengths in excess of 30 μm, which is an ideal size range for single molecule polymer dynamics. For single molecule studies, polydisperse samples can be easily analyzed, because the experimenter can select "targeted" polymer chains with specific contour lengths when acquiring data, which overcomes issues with chain length distributions. Alternatively, monodisperse samples of ssDNA can be obtained by denaturing monodisperse pieces of λ-DNA or other dsDNA. This approach has its own challenges, including labeling the polymer backbone with fluorescent dye without using modified nucleotides, and the possibility for base pairing and stacking due to lack of control over the sequence. Although the contour lengths of ssDNA molecules in this work are similar to λ-DNA, ssDNA is extraordinarily flexible. Whereas λ-DNA contains ~150 Kuhn steps, ssDNA contains ~10^4 Kuhn steps for a chain of similar contour length, assuming a bare persistence length of ~0.62 nm for ssDNA with screened electrostatic interactions[25].

3.4 Concluding Remarks

This chapter describes the labeling, quantification and visualization of single ssDNA molecules synthesized via rolling circle replication. The labeling reaction appears to proceed efficiently, and clear images of stretched ssDNA molecules were obtained using fluorescence microscopy. Labeling ratios for ssDNA are approximately 20 times less than that for λ-DNA, however fluorescent images of ssDNA were of similar quality. Due to the low dye labeling ratio, there was no evidence of dye-dye stacking interactions based on a nuclease assay. Therefore, we believe that our labeling scheme does not alter the backbone structure of the polymer chains, and the dynamic properties of the molecules are not expected to be perturbed from the native state.

In addition to direct imaging of single ssDNA molecules stretching in flow, the gel electrophoresis results for the synthesis reactions in Chapter 2 were also confirmed. A large number of stretched molecules appeared to be in excess of 20 microns (34 knt) in length. Ideally, for future dynamic experiments, having polymer chains with longer contour lengths is crucial for observing stretching pathways and relaxation time behavior at different degrees of extension. The polydispersity of the sample (Figure 12) can be overcome with careful trapping of molecules, allowing the experimenter should be able to "hand pick" molecules from a certain subset of lengths. There are also additional purification procedures such as gel extraction and gel-filtration chromatography that can be used to obtain a narrower distribution of polymer chain lengths.

Chapter 4
Conclusions

4.1 Concluding Remarks

In this work, the field of single molecule polymer dynamics studies has been extended to a new class of materials. Although λ-DNA has served as a model system for single polymer studies over the last several years, dsDNA is a semiflexible polymer chain with distinct local molecular properties. Here, ssDNA is presented as a new model system to study single flexible chains and polyelectrolytes. A straightforward synthesis technique based on rolling circle replication was developed to generate long strands of fluorescently-labeled ssDNA. Dye labeling is achieved using covalent dye incorporation, providing enhanced robustness to solvent conditions including low or high salt concentrations, thereby avoiding complications associated with using intercalating dyes in variable solvents. Precise control over ssDNA sequence will enable systematic investigation of the effect (if any) of DNA sequence on polymer chain dynamics. Additionally, reasonable product yields (5 μg labeled sample) allow for repeated use (100-200 experiments) of the same sample in single molecule work.

4.2 Future Directions

The ssDNA platform described here will enable a host of single molecule studies of polymeric materials. Template-based synthesis will allow for copolymers to be generated via chemical alteration of polymer backbones. End-functionalized primers for RCR will enable surface tethering for force extension measurements or synthesis on a surface. Surface based synthesis will allow for the study of polymer "brushes" and can provide

useful information regarding the dynamic behavior of concentrated polymer solutions. In addition to these materials-based applications, fluorescently-labeled ssDNA can be useful for biological systems. In one possible application, ssDNA "curtains" [45, 46] can be synthesized in microfluidic devices, facilitating high-throughput measurements of nucleic acid enzymology and protein-DNA interactions.

In the immediate future, the focus will shift from synthesis to measurement of dynamic properties of flexible polymers. More specifically, we will measure the longest relaxation time and stretching dynamics in an extensional flow for the ssDNA model system presented here. This work will highlight the differences between flexible and semiflexible chain behavior and could prompt a flurry of activity in the area of single molecule polymer studies.

References

1. Doi, M. and S.F. Edwards, *The Theory of Polymer Dynamics*. 1986: Oxford University Press.
2. Larson, R., *The Structure and Rheology of Complex Fluids*. 1999: Oxford University Press.
3. Shaqfeh, E.S.G., *The dynamics of single-molecule DNA in flow.* Journal of Non-Newtonian Fluid Mechanics, 2005. **130**(1): p. 1-28.
4. Perkins, T.T., et al., *Relaxation of a Single DNA Molecule Observed by Optical Microscopy.* Science, 1994. **264**(5160): p. 822-826.
5. Smith, D.E., T.T. Perkins, and S. Chu, *Dynamical scaling of DNA diffusion coefficients.* Macromolecules, 1996. **29**(4): p. 1372-1373.
6. Perkins, T.T., et al., *Stretching of a Single Tethered Polymer in a Uniform-Flow.* Science, 1995. **268**(5207): p. 83-87.
7. Jendrejack, R.M., J.J. de Pablo, and M.D. Graham, *Stochastic simulations of DNA in flow: Dynamics and the effects of hydrodynamic interactions.* Journal of Chemical Physics, 2002. **116**(17): p. 7752-7759.
8. Perkins, T.T., D.E. Smith, and S. Chu, *Single polymer dynamics in an elongational flow.* Science, 1997. **276**(5321): p. 2016-2021.
9. Smith, D.E. and S. Chu, *Response of flexible polymers to a sudden elongational flow.* Science, 1998. **281**(5381): p. 1335-1340.
10. Smith, D.E., H.P. Babcock, and S. Chu, *Single-polymer dynamics in steady shear flow.* Science, 1999. **283**(5408): p. 1724-1727.
11. Hur, J.S., et al., *Dynamics and configurational fluctuations of single DNA molecules in linear mixed flows.* Physical Review E, 2002. **66**(1): p. -.
12. Schroeder, C.M., et al., *Observation of polymer conformation hysteresis in extensional flow.* Science, 2003. **301**(5639): p. 1515-1519.
13. Balducci, A., C.C. Hsieh, and P.S. Doyle, *Relaxation of stretched DNA in slitlike confinement.* Physical Review Letters, 2007. **99**(23): p. -.
14. Balducci, A., et al., *Double-stranded DNA diffusion in slitlike nanochannels.* Macromolecules, 2006. **39**(18): p. 6273-6281.
15. Jendrejack, R.M., et al., *Effect of confinement on DNA dynamics in microfluidic devices.* Journal of Chemical Physics, 2003. **119**(2): p. 1165-1173.
16. Tang, J., D.W. Trahan, and P.S. Doyle, *Coil-Stretch Transition of DNA Molecules in Slitlike Confinement.* Macromolecules, 2010. **43**(6): p. 3081-3089.
17. Rubinstein, M. and R.H. Colby, *Polymer Physics*. 2003: Oxford University Press.
18. Bustamante, C., et al., *Entropic Elasticity of Lambda-Phage DNA.* Science, 1994. **265**(5178): p. 1599-1600.
19. Marko, J.F. and E.D. Siggia, *Stretching DNA.* Macromolecules, 1995. **28**(26): p. 8759-8770.
20. Hiemenz, P.C. and T.P. Lodge, *Polymer Chemistry*. 2 ed. 2007: CRC Press.
21. Quake, S.R., H. Babcock, and S. Chu, *The dynamics of partially extended single molecules of DNA.* Nature, 1997. **388**(6638): p. 151-154.

22. Jendrejack, R.M., M.D. Graham, and J.J. de Pablo, *Hydrodynamic interactions in long chain polymers: Application of the Chebyshev polynomial approximation in stochastic simulations.* Journal of Chemical Physics, 2000. **113**(7): p. 2894-2900.
23. Pincus, P., *Excluded Volume Effects and Stretched Polymer-Chains.* Macromolecules, 1976. **9**(3): p. 386-388.
24. McIntosh, D.B., N. Ribeck, and O.A. Saleh, *Detailed scaling analysis of low-force polyelectrolyte elasticity.* Physical Review E, 2009. **80**(4): p. -.
25. Saleh, O.A., et al., *Nonlinear Low-Force Elasticity of Single-Stranded DNA Molecules.* Physical Review Letters, 2009. **102**(6): p. -.
26. Zhao, W.A., et al., *Rolling circle amplification: Applications in nanotechnology and biodetection with functional nucleic acids.* Angewandte Chemie-International Edition, 2008. **47**(34): p. 6330-6337.
27. Reiss, E., R. Holzel, and F.F. Bier, *Synthesis and Stretching of Rolling Circle Amplification Products in a Flow-Through System.* Small, 2009. **5**(20): p. 2316-2322.
28. Daubendiek, S.L., K. Ryan, and E.T. Kool, *Rolling-Circle Rna-Synthesis - Circular Oligonucleotides as Efficient Substrates for T7 Rna-Polymerase.* Journal of the American Chemical Society, 1995. **117**(29): p. 7818-7819.
29. Fire, A. and S.Q. Xu, *Rolling Replication of Short DNA Circles.* Proceedings of the National Academy of Sciences of the United States of America, 1995. **92**(10): p. 4641-4645.
30. Liu, D.Y., et al., *Rolling circle DNA synthesis: Small circular oligonucleotides as efficient templates for DNA polymerases.* Journal of the American Chemical Society, 1996. **118**(7): p. 1587-1594.
31. Baner, J., et al., *Signal amplification of padlock probes by rolling circle replication.* Nucleic Acids Research, 1998. **26**(22): p. 5073-5078.
32. Blanco, L., et al., *Highly Efficient DNA-Synthesis by the Phage Phi-29 DNA-Polymerase - Symmetrical Mode of DNA-Replication.* Journal of Biological Chemistry, 1989. **264**(15): p. 8935-8940.
33. Buhot, A. and A. Halperin, *Effects of stacking on the configurations and elasticity of single-stranded nucleic acids.* Physical Review E, 2004. **70**(2): p. -.
34. Ke, C., et al., *Direct measurements of base stacking interactions in DNA by single-molecule atomic-force spectroscopy.* Physical Review Letters, 2007. **99**(1): p. -.
35. Mishra, G., D. Giri, and S. Kumar, *Stretching of a single-stranded DNA: Evidence for structural transition.* Physical Review E, 2009. **79**(3): p. -.
36. Seol, Y., et al., *Stretching of homopolymeric RNA reveals single-stranded helices and base-stacking.* Physical Review Letters, 2007. **98**(15): p. -.
37. Smith, S.B., Y.J. Cui, and C. Bustamante, *Overstretching B-DNA: The elastic response of individual double-stranded and single-stranded DNA molecules.* Science, 1996. **271**(5250): p. 795-799.
38. Goddard, N.L., et al., *Sequence dependent rigidity of single stranded DNA.* Physical Review Letters, 2000. **85**(11): p. 2400-2403.
39. Rief, M., H. Clausen-Schaumann, and H.E. Gaub, *Sequence-dependent mechanics of single DNA molecules.* Nature Structural Biology, 1999. **6**(4): p. 346-349.

40. Bommarito, S., N. Peyret, and J. SantaLucia, *Thermodynamic parameters for DNA sequences with dangling ends.* Nucleic Acids Research, 2000. **28**(9): p. 1929-1934.
41. Probes, M., *Aminoallyl dUTP*. 2004, Molecular Probes.
42. Cox, W.G., et al., *Possible sources of dye-related signal correlation bias in two-color DNA microarray assays.* Analytical Biochemistry, 2004. **331**(2): p. 243-254.
43. Carle, G.F., M. Frank, and M.V. Olson, *Electrophoretic Separations of Large DNA-Molecules by Periodic Inversion of the Electric-Field.* Science, 1986. **232**(4746): p. 65-68.
44. Olson, W.K. and J.L. Sussman, *How Flexible Is the Furanose Ring .1. A Comparison of Experimental and Theoretical-Studies.* Journal of the American Chemical Society, 1982. **104**(1): p. 270-278.
45. Graneli, A., et al., *Organized arrays of individual DIVA molecules tethered to supported lipid bilayers.* Langmuir, 2006. **22**(1): p. 292-299.
46. Greene, E.C., et al., *DNA Curtains for High-Throughput Single-Molecule Optical Imaging.* Methods in Enzymology, Vol 472: Single Molecule Tools, Pt A: Fluorescence Based Approaches, 2010. **472**: p. 293-315.